The Brookhaven ATF Low-Emittance Beam Line

X. J. Wang* and H. G. Kirk
Brookhaven National Laboratory
Upton, New York 11973

Abstract

One component of the experimental program at the Brookhaven Accelerator Test Facility (ATF) consists of a class of experiments which will study the acceleration of electrons through micron-size structures which are exposed in coincidence to a 100 GW CO_2 laser beam. These experiments require the development and control of an electron beam with geometric emittances on the order of 10^{-10}m-rad and intensities on the order of 10^6 electrons. In this paper, we describe the strategies for producing such beams and the effects of higher-order aberrations. Particle tracking results are presented for the final-focus system.

I. INTRODUCTION

The Brookhaven Accelerator Test Facility [1] is a facility dedicated to accelerator physics and FEL research and development. A pico-seconds, low-emittance electron beam is produced by a photocathode RF gun [2]. The electron beam is accelerated to 50 MeV by two sections of a SLAC type S-band linac.

The two major initial experiments at the ATF are a visible FEL [3] and laser acceleration experiments [4]. Due to budgetary and space constraints, the decision was made that the laser acceleration experimental beam line and the FEL beam line share as much as possible without compromising each experiment (Fig. 1). The ATF low-emittance beam line consists of an emittance-selection section, an achromatic transport section and a final-focusing system. We will describe each of these sections, study the higher-order effects on the beam emittance and the beam spot size produced by the final-focusing system.

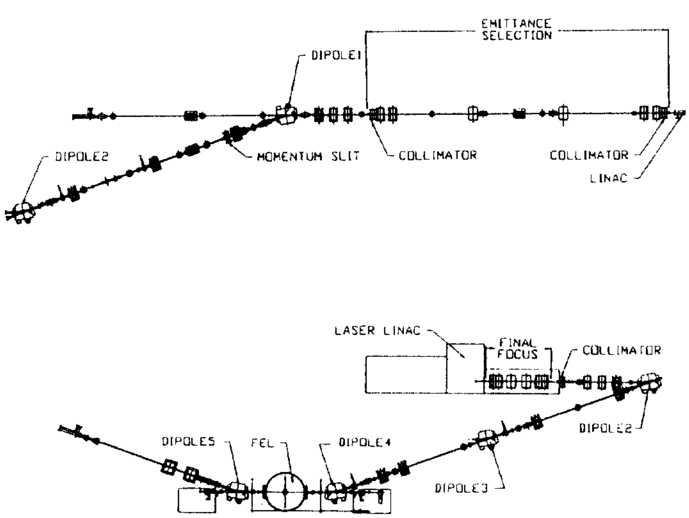

Fig. 1 ATF experimental beamline layout.

II. EMITTANCE SELECTION AND ACHROMATIC TRANSPORT LINES

The structures [4] used in the laser acceleration experiment require micron-size beams. This sets strict requirements for the final-focusing system and the emittance-selection section. The system chosen for the emittance-selection section produces the transverse beam parameters listed in Table 1. The emittance-selection line not only functions as an emittance selector, but also as a matching section for the FEL line.

Table 1. Beam parameters after the emittance-selection section.

$\varepsilon_x(mm-mrad)$	1.25×10^{-4}	$\varepsilon_y(mm-mrad)$	1.25×10^{-4}
x_{rms}(mm)	0.125	x'_{rms}(mrad)	0.001
y_{rms}(mm)	0.125	y'_{rms}(mrad)	0.001

We assume that the last triplet of the injection line [5] will produce a double beam waist 25 cm from the exit of the linac where the first collimator will be located. To achieve the emittance required, the phase ellipse has to be rotated $(2n+1)\frac{\pi}{2}$ at the second collimator. Following the TRANSPORT notation [6], the phase ellipse parameters at the second collimator are

$$\begin{aligned}\sigma_{11} &= R_{11}^2\sigma_{11}(0)+R_{12}^2\sigma_{22}(0)\\ \sigma_{22} &= R_{21}^2\sigma_{11}(0)+R_{22}^2\sigma_{22}(0)\\ \sigma_{12} &= R_{11}R_{21}\sigma_{11}(0)+R_{12}R_{22}\sigma_{22}(0)\,.\end{aligned} \tag{1}$$

A similar formula can be written for $y-y'$ phase space. The emittance selection demands $R_{11}=R_{22}=0$ and a large R_{12}. The emittance selected by the beam line is

$$\varepsilon=\frac{\sigma_{11}(0)}{R_{12}}. \tag{2}$$

An antisymmetric beam line consisting of six quadrupoles can satisfy the above conditions simultaneously in both x and y phase spaces.

We also consider the emittance growth caused by the chromatic effect. The emittance growth due to the chromatic effect of a quadrupole can be estimated by [5],

$$\Delta\varepsilon=\frac{<x^2>}{f}\left(\frac{\Delta P}{P_0}\right), \tag{3}$$

where f is the focal length of the quadrupole. Other parameters which play a large rule in deciding R_{12} are the drift distances before and after the third quadrupole.

* Center for Advanced Accelerator Physics, UCLA

0-7803-0135-8/91$01.00 ©IEEE

Generally speaking, the longer those drift distances are, the larger R_{12}. Our parameters were chosen so that the emittance growth is minimized. The total length of the emittance selection line is about 7 m. Fig. 2 shows the beam envelopes of the emittance-selection section.

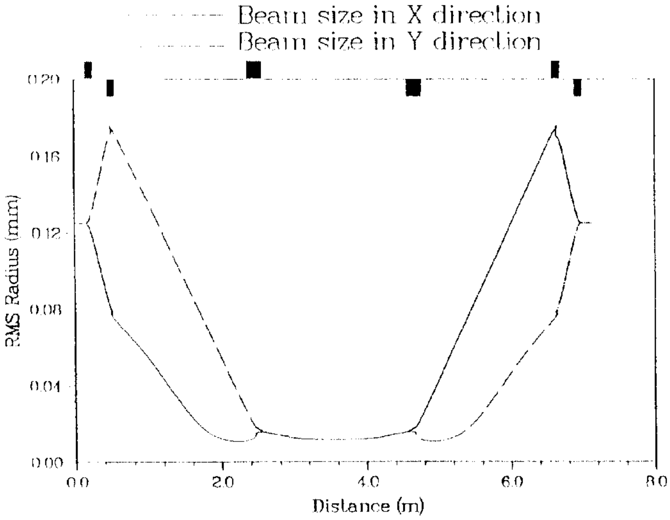

Fig. 2 The emittance selection line beam envelope.

The next section of the laser linac beam line transports the collimated electron beam from the second collimator to the experiment area with an $n\pi$ phase advance in both transverse dimensions and includes energy selection. In the transport line, there are not only chromatic effects, but also geometric effects from the dipoles. It is very important to keep the beam line symmetric and the beam sizes small so that emittance growth caused by all these effects is minimized. We have studied two versions of a telescopic system. Since the beam after the emittance selection is almost parallel, we first consider a quasi-telescopic system, which produces a parallel-to-parallel image. Fig. 3 shows the plots of beam envelopes and dispersion for this solution.

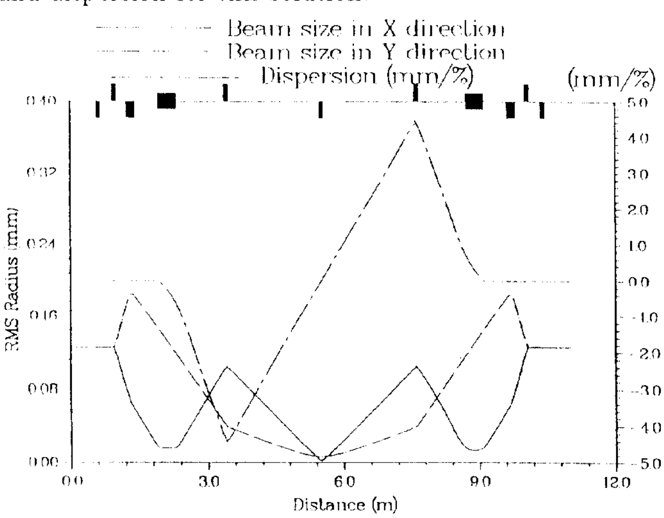

Fig. 3 The quasi-telescopic system beam profiles.

Our quasi-telescopic system will image a parallel beam into a parallel beam. For $R_{11} = R_{22} = -1$, and $R_{12} \neq 0$ the phase ellipse will be tilted from the upright position by $\theta = r_{12}\sqrt{\sigma_{22}/\sigma_{11}}$, where σ_{22} and σ_{11} are the phase ellipse parameters at the second collimator. They are 1.0×10^{-6} and 1.56250×10^{-2}, respectively. r_{12} is about 1, so the angle between the upright phase ellipse and our imaging ellipse is about 0.5 degrees.

We now consider a -I telescopic system, which can simultaneously produce a parallel-to-parallel and a point-to-point image. The beam envelopes and dispersion for such a system are plotted in **Fig.** 4.

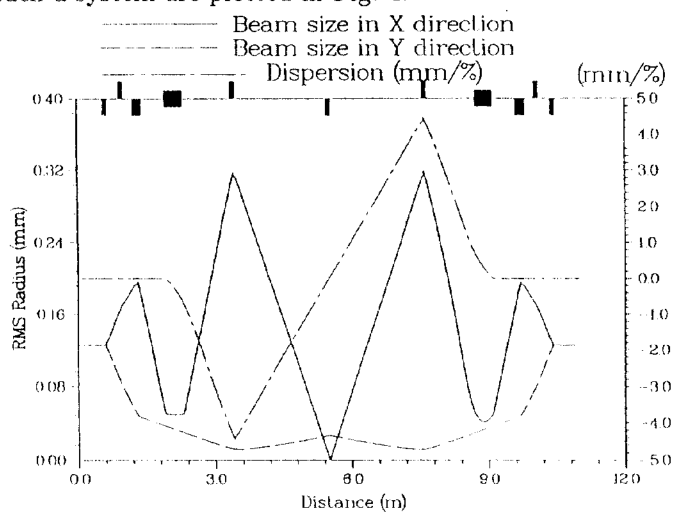

Fig. 4 The -I telescopic line beam profiles.

Comparing the two designs, the telescopic system is better from an optics point of view, but has larger horizontal beam dimensions which limits the energy selection and therefore exhibits a larger emittance increase. The quasi-telescopic system is able of providing better energy selection. In summary, our achromatic beam line can operate in two modes, the mode of operation depending on the energy selection requirement and the emittance of the beam being transported to the experimental area.

III. FINAL-FOCUSING SYSTEM

The last section of the laser linac beam line is the final-focusing system, which will produce a micron beam for laser acceleration experiments.

We first consider a telescope type final-focusing system, which consists of two quadrupole triplets. The spot size can be estimated for such a system (without sextapole correction) by [7]

$$\beta(\delta)_{min} \geq 8\ell^{*}\sigma_{\delta}, \tag{4}$$

where $\delta = \Delta p/p_0$ and $\ell^{*} \simeq 0.4$ m (determined by the dimension of the target box) is the drift distance between the last triplet and the target. For an emittance of 1.25×10^{-10} m-rad beam and $\sigma_\delta = 0.1\%$, the beam size is about 0.63×10^{-6} m, which satisfies the experimental requirements. But the space required for such a system is very large. Assuming the emittance-selection line can produce a spot size of 0.125 mm, then a demagnification factor $M \simeq 1/250$ is needed and the drift distance before the final-focusing system must be $\simeq M \times \ell^{*}$. This problem can be reduced by multistage focusing systems, but it still takes too much space.

The final-focusing system we have adopted has a character similar to our emittance selection line. It is a paralell-to-point imaging system. Instead of the large R_{12} of the emittance-selection section, a small R_{12} is required for our final-focusing system. The optimized design of our final-focusing system has a physical dimension of about 2 m (Table 2). The beam envelopes are plotted in Fig. 5.

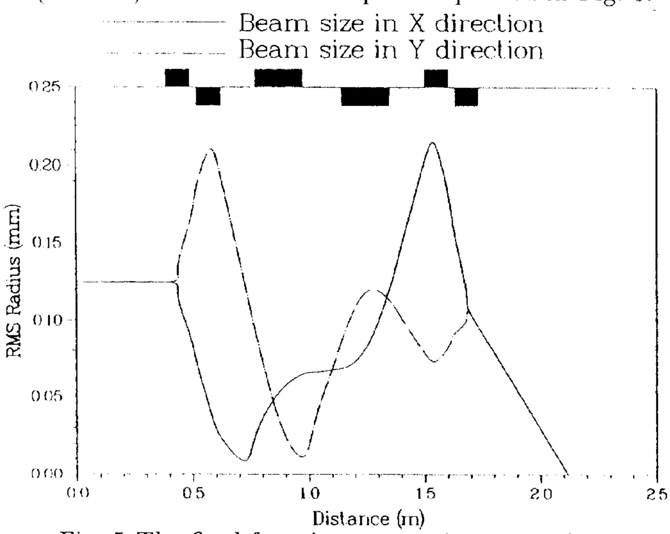

Fig. 5 The final focusing system beam envelope.

Table 2. Final-focusing system beam line elements parameters

	Length cm	Gradient Kg/cm
Drift	38.5	
Quad	10.2	0.93672
Drift	3	
Quad	10.2	-1.17811
Drift	15	
Quad	20.4	0.49447
Drift	17	
Quad	20.4	-0.49447
Drift	15	
Quad	10.2	1.17811
Drift	3	
Quad	10.2	-0.93672
Drift	38.5	

Using a thin lens approximation, the paralell-to-point imaging system can be represented by the following transfer matrix

$$R = \begin{pmatrix} 1-\frac{\ell^*}{f} & 2\ell^* - \frac{\ell^{*2}}{f} \\ -\frac{1}{f} & 1-\frac{\ell^*}{f} \end{pmatrix}. \qquad (5)$$

When $\ell^* = f$, then $R_{11} = R_{22} = 0$, $R_{12} = \ell^*$ and the focus spot is $\sigma_{11} = \ell^{*2}\sigma_{22}(0)$.

To consider the chromatic effect, substitute f by $\ell^*(1+\delta)$. The focus spot size is

$$\sigma_{11} = \ell^{*2}\sigma_{22}(0)(1+\delta)^2 + \sigma_{11}(0)\delta^2. \qquad (6)$$

We use a tracking program [8] to study how the spot size changes with different energy spreads. The results are shown in Fig. 6.

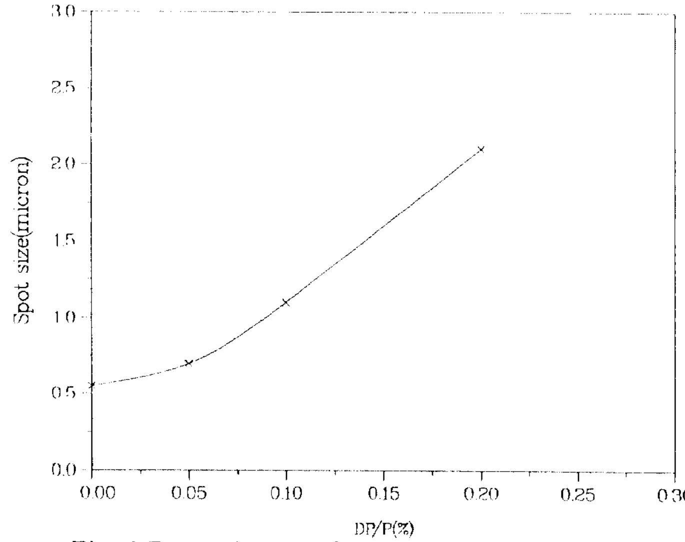

Fig. 6 Beam size as a function of enegy spread.

It can be seen from Fig. 6 that in order to have a spot size below one micron, the rms energy spread must be kept smaller than 0.1%. For the beam currents considered for the laser acceleration experiments, wake field and transient beam loading effects have no effect on the energy spread. The energy spread will be determined by the bunch length and the RF phase stability. The short electron bunch produced by the ATF injection system and the feed-forward control system [9] should be able to produce an electron beam whose energy spread will be smaller than 0.1%.

IV. CONCLUSION

We have presented a beam line for the laser acceleration experiments at the ATF which will produce a micron-size beam.

This work is supported by the U.S. D.O.E.

REFERENCES

[1] K. Batchelor, *et al.*, p. 540, 1988 Linear Accelerator Conference Proceedings.

[2] K. Batchelor, *et al.*, European Particle Accelerator Conference, 1988.

[3] K. Batchelor, *et al.*, Nucl. Inst. and Meth. **A296**, 239(1990).S

[4] R.C. Fernow *et al*, PROPOSAL for a Study of Laser Acceleration of Electrons using Micrograting Structures at the ATF.

[5] X.J. Wang, *et al.*, Proceeding of 1989 PAC, Chicago, March, 1989.

[6] TRANSPORT MANUAL, CERN 80 - 04.

[7] Karl L. Brown, p.481, Frontiers of Particle Beams, Eds by M. Month and S. Turner.

[8] X.J. Wang, BNL REPORT - 43101.

[9] I. Ben-Zvi, J.L. Xie and R. Zhang, these proceedings.